Proteomics and Electron Microscopic Characterization of the Unusual Mitochondrial Ribosome-Related 45S Complex in *Leishmania Tarentolae*

Dmitri A. Maslov[a,*], **Linda L. Spremulli**[b], **Manjuli R. Sharma**[c], **Kalpana Bhargava**[b], **Domenick Grasso**[b], **Arnold M. Falick**[d], **Rajendra K. Agrawal**[c,e], **Carol E. Parker**[f], and **Larry Simpson**[g]

a Department of Biology, University of California, Riverside, CA 92521, USA

b Department of Chemistry, University of North Carolina, Chapel Hill, NC 27599, USA

c Division of Molecular Medicine, Wadsworth Center, NY State Department of Health, Albany, NY 12201, USA

d Howard Hughes Medical Institute Mass Spectrometry Laboratory and Department of Molecular and Cell Biology, University of California, Berkeley, CA 94720, USA

e Department of Biomedical Sciences, State University of New York at Albany, Albany, NY 12201, USA

f North Carolina -Duke Proteomics Center, Department of Biochemistry and Biophysics, University of North Carolina, Chapel Hill, NC 27599, USA

g Department of Microbiology, Immunology and Molecular Genetics, University of California, Los Angeles, CA 90095, USA

Abstract

A novel type of ribonucleoprotein (RNP) complex has been described from the kinetoplast-mitochondria of *Leishmania tarentolae*. The complex, termed the 45S SSU*, contains the 9S small subunit rRNA but does not contain the 12S large subunit rRNA. This complex is the most stable and abundant mitochondrial RNP complex present in *Leishmania*. As shown by tandem mass spectrometry, the complex contains at least 39 polypeptides with a combined molecular mass of almost 2.1 MDa. These components include several homologs of small subunit ribosomal proteins (S5, S6, S8 S9, S11, S15, S16, S17, S18, MRPS29); however, most of the polypeptides present are unique. Only a few of them show recognizable motifs, such as protein-protein (coiled-coil, Rhodanese) or protein-RNA (pentatricopeptide repeat) interaction domains. A cryo-electron microscopy examination of the 45S SSU* fraction reveals that 27% of particles represent SSU homodimers arranged in a head-to-tail orientation, while the majority of particles are clearly different and show an asymmetric bilobed morphology. Multiple classes of two-dimensional averages were derived for the asymmetrical particles, probably reflecting random orientations of the particles and difficulties in correlating these views with the known projections of ribosomal complexes. One class of the two-dimensional averages shows an SSU moiety attached to a protein mass or masses in a monosome-like appearance. The combined mass spectrometry and electron microscopy data thus indicate that the majority 45S SSU* particles represents a heterodimeric complex in which the SSU

*Corresponding author. Tel: +1-951-827-6485; fax: +1-951-827-4286. *E-mail address*: maslov@ucr.edu (D.A. Maslov)

of the *Leishmania* mitochondrial ribosome is associated with an additional protein mass. The biological role of these particles is not known.

1. Introduction

Protein synthesis in trypanosomatid mitochondria is noted for its very unusual features that distinguish it from the translational systems in other organisms or subcellular organelles. The transcripts of a number of the mitochondrial genes encoded in the trypanosomatid mitochondrial DNA must be edited by U-insertions/deletions [1-3]. The mechanism that allows immature mRNA templates to be excluded from the translational machinery is unknown. Furthermore, how the ribosomes recognize the start site for protein synthesis is quite unclear. No Shine-Dalgarno sequence or equivalent signal is found upstream of the initiation codon. In contrast to mammalian mitochondria, the first AUG or AUA codon at the 5' end of the mRNA is generally not used as the start codon in trypanosomatid mitochondria [4-9]. Non-canonical initiation codons may also be used in some cases [7,10-13].

The complex nature of template recognition in trypanosomatid mitochondria is reflected in the unusual, complex structure of the protein biosynthetic apparatus in this organelle. In spite of extensive efforts made in the past, trypanosomatid mitochondrial ribosomes have proven very difficult to isolate and characterize [14-17]. The ribosomes from this organelle have substantially less RNA than do most ribosomes. The small subunit (SSU) contains a 9S rRNA while the large subunit (LSU) contains a 12S rRNA. Both of these are encoded in the mitochondrial genome [18-20]. These values are in contrast to bacterial ribosomes, which have a 16S rRNA in the small subunit and a 23S rRNA in the large subunit. The trypanosomatid rRNAs are also smaller than those present in mammalian mitochondria (12S in the SSU and 16S in the LSU) [21]. The small size of the rRNAs indicates that the trypanosomatid ribosome is a protein-rich particle.

We have recently described several rRNA-containing ribonucleoprotein complexes from the mitochondria of *Leishmania tarentolae*, including putative 50S monosomes, 40S large subunits and ~30S small subunits [22]. In addition, an unusual ribosomal RNP complex, termed 45S SSU*, was found [22]. This stable and abundant complex contained the small subunit 9S rRNA and several homologs of small subunit ribosomal proteins. As revealed by negative staining electron microscopy, the complex had a bilobed morphology and was clearly different from the ~30S small subunits which were found in low abundance. Morphologically the 45S complex was reminiscent of 50S monosomes; however, it was clearly different from monosomes due to the lack of the LSU rRNA. We hypothesized that the 45S SSU* complexes represent homodimers of the 30S small subunits or a complex of the SSU with an unidentified large protein complex. To achieve better insight into the nature and potential role of the 45S SSU* complexes we have undertaken a detailed mass spectrometry and electron microscopy (EM) analysis of these complexes.

2. Materials and methods

2.1. Cell growth and fractionation

Cultivation of *L. tarentolae* (UC strain) and isolation of the kinetoplast-mitochondrial fraction was carried out by the hypotonic procedure described previously (ref. [22] and references therein).

2.2. Isolation of the 45S SSU* ribosomal RNP complexes

Initially, purified mitochondria ($\sim$ 1 g, wet weight) were lysed on ice for 1 h with 20-25 mL of buffer containing 0.2% NP40 (IGEPAL® CA-630, Sigma), 50 mM Tris-HCl, pH 7.5, 100 mM KCl, 10 mM MgCl$_2$, 3 mM DTT and 0.1 mM EDTA [16]. Subsequently, NP40 was replaced with a different non-ionic detergent, dodecyl maltoside, which is equally efficient for membrane solubilization but has less effect on protein-protein interactions, and lysis conditions were modified as described previously [22]. Ribosomal RNP complexes were recovered from the cleared mitochondrial lysate by sedimentation through a 1.1 M sucrose cushion prepared in SGB100 buffer (50 mM Tris-HCl, pH 7.5, 100 mM KCl, 10 mM MgCl$_2$, 3 mM DTT, 0.1 mM EDTA and 0.05% dodecyl maltoside) or SGB500 buffer (of the same composition, except that the concentration of KCl was 500 mM). Centrifugation was performed at 28,000 rpm (RCF$_{avg}$ = 55,700 $\times$ g) for 20 h in a Type 60Ti rotor unless specified otherwise. Each tube contained 10 mL of the lysate and an equal volume of the cushion buffer. The pellets were resuspended in SGB100 buffer supplemented with 1% dodecyl maltoside (1 mL of the buffer per pellet), kept on ice for 1-2 h and centrifuged at 14,000 $\times$ g to remove the insoluble material. The supernatant containing solubilized complexes was then fractionated in a 7-30% linear sucrose gradient in an SW28 rotor at 20,000 rpm (RCF$_{avg}$ = 52,900 $\times$ g) for 16 h. Fractions were analyzed for the quantity of the 9S SSU and 12S LSU rRNA as described previously [22]. The 45S SSU* complexes were recovered by sedimentation at 200,000 $\times$ g for 2 h and then fractionated in a second gradient centrifugation as described previously [22].

To obtain the high salt-washed 45S SSU* fraction, mitochondria were lysed with 0.2% NP40 in the buffer containing 50 mM Tris-HCl, pH 7.5, 500 mM KCl, 0.1 mM MgCl$_2$, 3 mM DTT, 0.1 mM EDTA. The sucrose cushion and the gradients were done with the same buffer except that the concentration of KCl was 400 mM (cushion) or 1.5 M KCl (gradients) and the concentration of NP40 was 0.05%.

2.3. Protein electrophoresis

Proteins in gradient fractions were analyzed in 12% Tris-glycine-SDS polyacrylamide gels [23]. Fraction material (up to 50 μL) was mixed with an equal volume of the sample buffer [24], incubated at 55 °C for 15 min and applied to the gel. Alternatively, proteins from the gradient fractions were precipitated by the addition of 20% of a solution containing 100% (weight per volume) trichloroacetic acid and 0.5% deoxycholate. The precipitated material was recovered by centrifugation at 14,000 $\times$ g for 40 min, washed with 100% acetone, air dried, dissolved in a small (5-20 μL) of the sample buffer and analyzed in 8-16% gradient Novex® Tris-glycine gels (Invitrogen). Gels were stained with Colloidal Blue Coomassie® stain or SYPRO® Ruby stain (Invitrogen).

2.4. Mass spectrometry

Monomeric and dimeric 45S SSU* complexes obtained in 100 mM KCl were sedimented by high speed centrifugation and resuspend in 25 mM ammonium bicarbonate. Samples (about 5 μg) were digested with trypsin as described previously [22]. The resulting peptides were dissolved in 20 μL aqueous 5% acetonitrile and 0.1% formic acid and analyzed by liquid

chromatography tandem mass spectrometry (LC MS/MS). The system used a Waters/ Micromass API US Q-TOF mass spectrometer, interfaced to Waters CapLC. The HPLC system consisted of a 5 mm × 800 Å id C18 P3 trapping column and a 15 cm × 75 μ id C18 PepMap analytical column (Dionex Corporation). MS spectra were obtained using the "survey" mode in which an MS scan is first acquired, followed by MS/MS scans on parent ions that meet a preselected intensity threshold. The intensity threshold was set to the minimum allowable value of "1" for these experiments. MS spectra were acquired over a mass range from 400 to 1900, and MS/MS spectra were acquired over the mass range 50 to 1900, using a scan rate of 1 s/ scan. To create MS/MS spectra (peak lists) from the data, the Waters/Micromass ProteinLynx software (version 2.0) was used. These peak lists were analyzed using our site-licensed Mascot database searching program [25] (www.matrixscience.com), in which the *L. major* protein and EST databases had been installed. This database was supplemented with the sequence of the mitochondrially encoded small subunit ribosomal protein S12 which was not present in the original database list. The observed MS/MS spectra were matched against spectra from a theoretical digest of all of the proteins in the database to provide candidate proteins. Individual ion scores of greater than 26 indicate identity or extensive sequence similarity (p<0.05) when MS/MS data are queried against the *L. major* database. This criterion is somewhat strict since the peptides are actually derived from *L. tarentolae*. Only those peptides with this level of stringency were considered in the summary provided in Table 1. Note that the Mascot score is a probability based MOWSE score [26]. The total Mascot score and the range of individual ion scores for the peptides are provided in Supplementary Tables 1 and 2.

Proteins in the complexes obtained in high salt conditions were separated by SDS-polyacrylamide gel electrophoresis. The bands were excised, digested *in situ* with trypsin and analyzed by MALDI tandem mass spectrometry (MALDI MS/MS) as described previously [22]. The MALDI MS/MS spectra were interpreted manually and the matched sequences were searched in the *L. major* database using the built-in BLAST program.

The peptide-matching regions in the identified proteins are summarized in Supplementary Table 3.

2.5. Cryo-electron microscopy

Cryo-EM grids of the 45S complexes were prepared according to standard procedures [27]. Data were collected on a Philips FEI (Eindhoven, The Netherlands) Tecnai F20 FEG microscope, equipped with low-dose kit and an Oxford cryo-transfer holder, at a magnification of 50,760-fold between 2.0 and 4.5 μm under focus range. From a total of 128 micrographs, the110 best ones were scanned on a Zeiss flatbed scanner, with a step size of 14 μm, corresponding to 2.76 Å on the object scale. From the originally windowed 24,826 images from the scanned micrographs, 12,678 images were manually selected and subjected to reference-free alignment and two-dimensional correspondence analysis [28] using SPIDER [29].

2.6. Protein sequence analyses

Routine analyses were performed using Vector NTI version 9.0. Structural domains were searched on-line using SMART (smart.embl-heidelberg.de/) and PROSITE (ca.expasy.org/ prosite/). Database similarity searches were performed using NCBI BLASTP 2.2.14 (release of May 7, 2006). Mitochondrial localization was predicted using MitoProt (ihg.gsf.de/ihg/ mitoprot.html).

3. Results

3.1. Isolation of the 45S SSU* complexes for mass-spectrometry

Earlier work demonstrated that when high molecular weight complexes prepared from *Leishmania* mitochondrial lysates by high speed sedimentation were fractionated in a sucrose gradient, the bulk of the 9S and 12S rRNA was observed sedimenting in the ∼50S region of the gradient. Three types of ribonucleoprotein complexes were identified in this region: 40S large subunits (LSU), 45S SSU-related complexes (45S SSU*) and 50S putative monosomes [22]. The pelleting step reduces the amount of the free LSU complexes (Fig. 1 compared to Fig. 1A of ref. [22]). This behavior of the large subunits is unusual since sedimentation at high speeds is commonly used for the isolation of ribosomes from various sources [30]. However, RNP particles, especially the large subunit of the ribosome, in *Leishmania* mitochondria, are destabilized and tend to aggregate during this treatment. The 45S SSU* complexes are, however, not strongly affected by sedimentation. This property has facilitated their isolation largely free of other RNP complexes (data not shown).

The procedure developed for isolation of the 45S SSU* complexes was similar to the procedure described previously [22] except that sedimentation of ribosomal RNP complexes through a sucrose cushion was used to selectively reduce contamination with the large subunits and other particles. Monomeric 45S complexes from several sucrose gradients similar to the one shown in Fig. 1 were pooled, recovered by centrifugation and then fractionated in a second sucrose gradient (Fig. 2A). The RNA profile showed two peaks of the 9S SSU rRNA representing the initial monomeric 45S complexes and the spontaneously formed dimeric 70S complexes, as described previously [22]. The 12S LSU rRNA content in such gradients was very low. As revealed by conventional, negative-stain transmission EM (Fig. 2B), the 45S fraction was predominantly composed of asymmetrical bilobed complexes as also observed previously (compare with Fig. 3A of ref. [22]). A few smaller round-shaped particles were also seen (indicated with arrows in Fig. 2B). The structures may represent contaminating F_1F_0 ATP synthase.

The monomeric and dimeric complexes were recovered by pelleting. Analysis of the protein composition of the 45S SSU* complexes by SDS-polyacrylamide gel electrophoresis (Fig 2C) revealed a specific pattern of polypeptide bands. These polypeptides ranged in size from 15 to 190 kDa. The cofractionation of these protein bands with the 9S rRNA was reproducible and was observed under a variety of lysis conditions with or without a prior sedimentation step. A similar pattern of protein bands was observed in the 70S region of the gradient in agreement with the observation that the 70S particles represent a dimeric form of the 45S SSU* RNP (Fig. 2C).

To assess which protein bands observed (Fig. 2C) represented integral components of the 45S and 70S SSU* complexes and which might be loosely associated with these RNPs, mitochondria were lysed and the RNP complexes were purified in buffers containing elevated concentrations of salt. For this process, ribonucleoprotein complexes from the mitochondrial lysate were pelleted through a sucrose cushion containing 400 mM KCl and 0.1 mM $MgCl_2$. They were then resuspended in buffer prepared with 1.5 M KCl and 0.1 mM $MgCl_2$ and fractionated in a sucrose gradient containing this high salt concentration. This treatment should remove proteins or RNA components loosely bound to the complex. The high salt treatment had a drastic effect primarily on the integrity of the 12S-containing complexes (Fig. 3A, upper panel), which almost completely disassembled in high salt forming free 12S rRNA. A large proportion of the 9S-containing complexes were destroyed as well. However, a prominent peak of the SSU* complex that sedimented somewhat slower than the original 45S complex was still observed. The material in the main SSU* complex was collected by sedimentation and

fractioned on a second high salt-containing gradient (Fig. 3A, lower panel). It was noteworthy that, in addition to the initial complex, the dimerization complex was observed under these conditions. The monomeric and dimeric SSU* material was recovered from several high salt gradients and combined. The protein content of this fraction (Fig. 3B) was very similar to that obtained under the lower salt conditions (Fig. 2C).

3.2. Tandem mass-spectrometry analysis of the 45S SSU* complexes

To assess the identity of the polypeptides associated with the 9S rRNA in the 45S and 70S RNP complexes, three SSU* preparations (the monomeric and the dimeric complexes obtained under normal conditions (Fig. 2C) and the high salt washed complexes (Fig. 3B)) were examined by mass spectrometry. Polypeptides in the first two fractions were digested with trypsin and the mixture of peptides was subjected to nanoscale capillary LC MS/MS. Components of the salt washed complexes were resolved using an 8-16% gradient polyacrylamide gel. The gel was cut into 43 segments to cover the polypeptide size range from 200 to 10 kDa. The polypeptides were digested with trypsin *in situ* and subjected to MALDI MS/MS. The combined list of the polypeptides identified in the *L. major* gene database is presented in Table 1. All identified proteins but one (LmjF24.0800) were also found in the gene databases of *Trypanosoma brucei* (www.genedb.org/genedb/tryp/) and *Trypanosoma cruzi* (www.genedb.org/genedb/tcruzi/).

The polypeptides found were classified into three categories. The first category ('high confidence hits') includes the 39 proteins that were present in all three of the SSU* preparations analyzed. These polypeptides were considered to be the *bona fide* components of the SSU* complexes (Table 1). The calculated molecular mass of the 45S SSU* complex containing a single copy of the 9S RNA and the set of 39 proteins is 2.08 MDa (this value also includes the predicted signal peptides because the cleavage sites were uncertain in some cases). This mass falls within the expected range for a complex with a sedimentation value of 45S. For comparison, the molecular mass of the 55S mammalian mitochondrial ribosome containing the 12S SSU rRNA, the 16S LSU rRNA and 77 proteins is 2.71 MDa [31].

In addition, 10 polypeptides were encountered in two preparations out of the three, and therefore, could also represent components of the particles. Their presence would increase the size of the complex to 2.46 MDa.

Several polypeptides were observed in a single preparation only (data not shown). These polypeptides were operationally regarded as contaminants, although some of them, especially small size molecules, still might represent authentic components of the 45S complexes. Among the likely contaminants were two LSU proteins, L15 and L21, found in the dimeric 70S preparation, which could be contaminated with dimeric LSU particles (65S), and L20 encountered in the salt washed particles. In addition, several abundant mitochondrial housekeeping enzymes and heat-shock proteins were frequently encountered during the analyses (data not shown). Thus, subunits of pyruvate dehydrogenase were seen in the salt washed complexes, while ATP synthase subunits were observed in the monomeric and dimeric 45S preparations. Superoxide dismutase and enoyl-CoA hydratase were encountered in all three preparations.

3.3. Homologs of small subunit ribosomal proteins

Seven homologs of small subunit ribosomal proteins identified earlier in the analysis of the mixed 45S/50S fraction (S5, S9, S11, S15, S16, S17, S18) and three additional components (S6, S8 and MRPS29) have been found in the 45S SSU* complexes. The degree of sequence conservation varies greatly among these polypeptides. Thus, the identification of the S5, S8,

S17 and MRPS29 homologs was based on BLAST searching that yielded highly significant E-values smaller than the conventional 1e-03 cut-off value.

Although the BLAST E-scores for the putative S11 were not significant (E ≥ 0.51), this *Leishmania* protein contains the RNAse H-like SCOP (Structural Classification of Proteins) domain (E = 3e-07) present in the ribosomal protein family including S11 and L18, as well as the NCBI conserved domain RpsK (representing ribosomal protein S11) (E = 0.0001). Similarly, the best BLAST E-score for the S9 homolog was only 0.12. Nonetheless, the identification of this protein is reliable: it was based on finding ribosomal protein S5 domain 2-like SCOP domain (E = 4e-16) present in the S5 and S9 ribosomal protein families; and finding the Ribosomal_S9 Pfam domain (E =0.0008). The S15 homolog was identified based on the similarity to putative mitochondrial S15 proteins from *Theileria annulata* (E=0.009) and *Schizosaccharomyces pombe* (E=0.037) and the presence of the S15/NS1 RNA binding SCOP domain (E=0.014).

The identification of the presumed S6, S16 and S18 homologs was not strongly supported. The putative S6 homolog was identified only by a weak similarity to several mitochondrial S6 proteins. The second protein was moderately similar to fungal MRPS24 (S16 family) (E ≥ 0.038). The third protein was found to contain the SCOP ribosomal protein S18 domain (1.80e-02) but demonstrated only a weak similarity to the corresponding eubacterial proteins.

Most of the identified small subunit ribosomal proteins were highly basic (pI > 9), as are their homologs in other sources, reflecting their interactions with the ribosomal RNA [32-35]. Mitochondrial ribosomal proteins, as a rule, are significantly longer than their eubacterial counterparts [31-38]. This difference is due to the presence of N- or C-terminal extensions which were proposed to serve structural and/or functional compensation for the missing stem-loop structures of the ribosomal RNAs [36], although this idea was not supported by the cryo-EM analysis of bovine mitoribosomes [31]. In *Leishmania*, the increase in length was due to long N-terminal extensions for several ribosomal proteins including S8, S9 and S11. Long C-terminal, as well as the N-terminal extensions are present on several other proteins (S5, S15, S17, S18). Two proteins (S6 and S16) were only slightly longer than the proteins from *E. coli*. In addition, six *Leishmania* polypeptides (S8, S11, S15, S16, S17, S18) were longer than their homologs in other mitochondria (Supplementary Table 4).

As summarized above, the proteomics analysis indicated the presence of 10 candidates for SSU proteins in the trypanosome SSU* complexes. This number is somewhat smaller than the 14 prokaryotic homologs found in the bovine mitochondrial 28S SSU. With the exception of S8, all of the homologs observed in *Leishmania* are also observed in mammalian mitochondrial ribosomes (Supplementary Tables 4 and 5). In general the similarity between the *Leishmania* SSU homologs and the bacterial proteins is somewhat higher than with homologs observed in other mitochondrial translational systems (Supplementary Table 5). This observation suggests that different constraints have been placed on the mitochondria of different organisms during evolution leading to considerable divergence in the ribosomal proteins.

3.4. Other components of the 45S complexes

Most of the polypeptides identified in this work did not show homology to SSU ribosomal proteins (Table 1). With the exception of the three pentatricopeptide repeat (PPR)-containing polypeptides, a member of the 2H 2',3' cyclic phosphodiesterase superfamily, and a DEAD-box helicase, the remaining polypeptides were devoid of nucleotide- or RNA-recognition motifs. Instead, several of these proteins contain motifs known to participate in protein-protein interactions. These include five polypeptides with coiled coil domains, a polypeptide with a

non-catalytic Rhodanese homology domain, a ubiquitin-like protein and a tetratricopeptide repeat (TPR)-containing protein. It is noteworthy, that these additional proteins were relatively large compared to the components usually found in ribosomes: the largest coiled coil protein was nearly 200 kDa in size while the largest mammalian mitochondrial ribosomal protein was 60 kDa [37]. Half of the 45S complex protein components were devoid of recognizable structural features.

Most of the proteins identified had a predicted mitochondrial localization signal (by TargetP and MitoProt) and cleavable signal peptides (data not shown). However for some of these, including the S9 and MRPS29 homologs, these features were not predicted. These mixed results point to the presence of diverse mitochondrial importation signals in trypanosomatids, with some of these signal types remaining unaccounted for.

3.5. Cryo-EM characterization of the 45S complexes

For the cryo-EM analysis, the monomeric 45S SSU* complexes were isolated under normal ionic conditions (100 mM KCl, 10 mM MgCl$_2$) in a sucrose gradient without a prior pelleting step. The complexes were purified in a second sucrose gradient (Fig. 4A). The contamination with the 12S-containing complexes (50S and 40S) in the 45S peak fractions was at a low level (<10% by the relative RNA content).

The manually selected 12,678 particle images were used to calculate nearly four hundred two-dimensional (2D) averages. About 40% of these averages represented recognizable views of the ribosomal particles and were categorized into three groups (Figs. 4B and 4C). The averages shown in panels B1-B4 in Fig. 4B, represented by ∼27% particle images, demonstrate bilobed features. The lobes have more or less cylindrical shape, readily identifiable with projection images of ribosomal SSUs. These averages represent SSU dimers in which the two SSUs appear to be situated side by side (as in the number 69). The averages shown in panels C1 and C2, represented by <1 % of single particle images, also show bilobed features, although clearly different from those in panels B1-B4. Those minor classes of particles match closely with the particles often observed by EM of the negatively-stained sample (Fig. 2B, see also Fig. 3 of ref. [22]). These averages, apparently, represent the views in which the two SSU particles are partially overlapping. The third class of averages, represented by ∼13% particle images (panels C3 and C4), also show asymmetrical bilobed features. These averages resemble the 2D averages of the 50S monosomes [22] with the clearly recognizable SSU presented in the upper right side and the LSU-like feature seen in the lower left. Yet, this feature could either represent an unfamiliar view of the SSU (originated due to a skewed orientation of one of the two SSUs on the cryo-EM grid), or a protein mass which is unrelated to both SSU and LSU. An additional possibility is that these classes of averages could represent the 12S rRNA-depleted monosome particles, however, this interpretation is inconsistent with the absence of LSU proteins in the 45S sample.

The majority (∼60%) of the analyzed particle images could not be easily correlated with the 40% described above. Rather, they were dispersed among various average classes with unfamiliar views (not shown), i.e., the views that could not be assigned to any known 2D class averages of monosomes or subunits. However, these complexes appear to contain a SSU in an unknown type of complex. The images obtained may represent orientations that are unique to SSU dimers, or they may represent complexes of the SSU with some additional protein masses.

4. Discussion

One of the most interesting observations made about the mitochondrial rRNAs in trypanosomatid mitochondria is their presence in unusual complexes that do not correspond to

the classical large and small ribosomal subunits observed in other translational systems. In particular the 9S rRNA is present not only in the putative 25S-30S SSU but also in the 45S SSU* complex. In the present report, we have used tandem mass-spectrometry and cryo-EM to help identify the nature of this unusual complex.

Tandem mass-spectrometry had been successfully applied to the analysis of the protein composition of ribosomes from several organelles including bovine mitochondria [32,33, 36-38], fungal mitochondria [39,40] and chloroplasts [41,42]. To reduce contamination by other large oligomeric complexes we have used preparations of the complexes obtained by different procedures, including monomers, spontaneously formed dimers and salt washed monomers. The rationale was that each type of preparation should be contaminated by different mitochondrial components, and only authentic components of the 45S complexes would be present in each preparation. In assessing the authenticity of the identified proteins, we have also taken into account that the most abundant mitochondrial complexes, such pyruvate dehydrogenase and ATP synthase, would almost certainly be present in each fraction obtained. Clearly, in the absence of a more detailed structural and functional characterization of each identified component, the composition of the 45S SSU* complexes described herein should be regarded only as a working model. The likely exceptions from this cautionary rule are the proteins homologous to small subunit ribosomal proteins from other organisms.

In assessing how complete the coverage of the SSU mitochondrial proteins obtained might be, we investigated whether any potential candidates with homology to known prokaryotic ribosomal proteins were present in the *Leishmania* genome. For this analysis, each of the eubacterial SSU proteins was BLAST-searched against the *Leishmania major* protein database. Hits were observed for most of the *E. coli* SSU protein queries. However, many of these hits resembled cytoplasmic ribosomal proteins. Next the sequences of the yeast cytoplasmic ribosomal proteins were BLAST-searched against the *Leishmania* protein database. The homologs of these proteins were readily detected in this analysis (Supplemental Table 6). Of these putative cytoplasmic ribosomal proteins, 13 were also homologous to the eubacterial proteins, albeit with a lower level of sequence similarity than to their cytoplasmic counterparts. Moreover, all of the hits, with one exception (S17) observed when *E. coli* ribosomal proteins were used as a query against the *Leishmania* gene database were cytoplasmic ribosomal proteins. Thus, it appears that the genome does not contain any typical mitochondrial SSU ribosomal proteins in addition to those found in the proteomics analysis. The one exception here is ribosomal protein S12 which is present in the mitochondrial genome rather than in the nuclear genome [9,43]. This small protein is generally entwined into the rRNA and may not have been digested adequately during the trypsin treatment to allow its detection. There is a homolog to prokaryotic S12 in the nuclear genome of *Leishmania* (LmjF13.0570). This protein has a strong mitochondrial import signal as predicted by MitoProtII. However, BLAST analysis indicated that this polypeptide is more similar to cytoplasmic S12 proteins than to bacterial S12 and this gene most likely encodes a component of the cytoplasmic ribosomes.

Many of the proteins found in the SSU* complex do not display a recognizable homology outside the Trypanosomatidae family and only a few of them have well-characterized functional domains (Table 1). Some of the unique proteins, especially the large size polypeptides with coiled coil domains, are likely to play structural roles in the complex. The presence of proteins with the sizes exceeding 60 kDa is unprecedented for a ribosomal RNP complex. It is plausible that these proteins compensate for a weak structural scaffold provided by the 9S rRNA.

The three proteins with pentatricopeptide domains and a DEAD/H-box helicase may be involved in RNA recognition. Hundreds of PPR proteins are found in plants where they are

thought to be involved in post-transcriptional gene regulation in organelles by specific binding to mRNA [44]. Recently, 23 conserved members of the PPR family were identified by a genome-wide search in *T. brucei*, and the down-regulation of one of these proteins had influenced steady-state levels and editing of some of the maxicircle gene transcripts [45]. One of the three PPR proteins present in the 45S complexes (LmjF24.0830) was not found in that work. An additional PPR protein (LmjF21.1620) was identified by a single hit in the dimeric 45S complexes (data not shown) but its relationship with the complex is unclear. The detected helicase is different from the mHel61 DEAD-box enzyme potentially implicated in RNA editing [46]. It is possible that the ribosomal PPR proteins and the helicase mediate interactions between mRNAs and translation machinery, but this hypothesis still needs to be investigated.

A component of the complex (LmjF32.0650) was found to contain a partial LigT domain. The full domains are present in members of the 2H cyclic phosphodiesterase (CPDase) superfamily which is defined by two Hh[S/T]h (where 'h' is a hydrophobic amino acid) motifs [47]. Only one such unit is present in the LmjF32.0650 protein, however, dimerization of the 45S complexes might bring two units together forming a CPDase active site. The function of this activity in the 45S complex is open to speculation. It is noteworthy that the *Leishmania* protein shows a meaningful sequence similarity (with E-values up to 3e-09) to mammalian AKAP7/ AKAP18 (activated protein kinase A anchoring protein) [48]. Thus, there is a possibility that a cAMP-dependent phosphorylation may be involved in regulation of a function of the 45S complex and that it is modulated by the LmjF32.0650 protein. It was shown that cAMP-dependent pathways are involved in regulation of oxidative phosphorylation complexes in other mitochondria [49-51].

While the conventional negative-stain EM showed a bilobed feature in a majority of the 45S particles (Fig. 2B and ref. [22]), the cryo-EM analysis has revealed a wide variety of 2D views of the 45S particles. This complexity could originate from a commonly observed preferred orientation and distortion of particles imaged by the negative staining method, compared to capturing all possible orientations of particles in their native conformation with the cryo-EM approach. The variety of 2D views described here was also due to morphological heterogeneity of the 45S complexes. A lobe with the SSU-like structural features could be readily identified in a significant proportion of the particle images. This structure likely contained the 9S SSU rRNA and SSU protein homologs. It must be stressed that it is unknown if this part is fully equivalent to the SSU as it would be found in functional monosomes. A significant portion (27%) of the all computed 2D averages (Fig. 4, panels C1-C4) were clear homodimers of this SSU-like structure, while the rest of particles had a different morphology. A portion of particles (13%) appeared monosome-like (Fig. 4, B3, B4). However, as pointed out earlier, it is unlikely that such particles represented contaminating LSU-containing monosomes, due to the absence of the LSU RNA and LSU protein homologs in the biochemical analysis of 45S complexes. We propose that the LSU-like appearance of one of the two lobes in the respective 2D averages arise mostly from unique additional protein masses attached to the SSU-like lobe. The remaining 60% of the analyzed particles represented more than 300 different 2D averages which appeared to show differently oriented complexes of SSU with additional protein masses or SSU dimers, and could not be easily correlated with the known projection of ribosomal complexes.

The number of proteins found in the 45S complexes (at least 39) and their combined mass (at least 2.08 MDa) are too high to be attributed to an SSU particle alone. This discrepancy is resolved by the presence of abundant heterodimeric particles composed of a single SSU lobe and an additional protein mass or masses. It is possible that many unique proteins identified by the proteomics analyses belong to the non-SSU lobe of the heterodimer. The significance of the sequestration of individual small subunits within a larger complex remains unclear. It is

possible that this may prevent an uncontrolled translation of immature pre-edited and partially edited mRNA. Alternatively, at least some of the polypeptides present in the 45S particles, in particular the PPR proteins, may be involved in template recognition. Further studies are necessary to shed light on these problems.

Supplementary Material

Refer to Web version on PubMed Central for supplementary material.

Abbreviations

cryo-EM, cryo-electron microscopy; DTT, dithiotreitol; LC, liquid chromatography; LSU, large subunit; MALDI, matrix-assisted laser desorption-ionization; MRP, mitochondrial ribosomal protein; MS, mass spectrometry; rRNA, ribosomal RNA; SSU, small subunit; TOF, time-of-flight.

References

1. Benne R, Van den Burg J, Brakenhoff J, et al. Major transcript of the frameshifted coxII gene from trypanosome mitochondria contains four nucleotides that are not encoded in the DNA. Cell 1986;46:819–26. [PubMed: 3019552]

2. Simpson, L.; Maslov, DA.; Blum, B. RNA Editing in Leishmania Mitochondria. In: Benne, R., editor. RNA Editing - the alteration of protein coding sequences of RNA. Ellis Horwood; 1993. p. 53-85.

3. Stuart, K. RNA editing in mitochondria of African trypanosomes. In: Benne, R., editor. RNA Editing - the alteration of protein coding sequences of RNA. Ellis Horwood; 1993. p. 25-52.

4. Bhat GJ, Koslowsky DJ, Feagin JE, et al. An extensively edited mitochondrial transcript in kinetoplastids encodes a protein homologous to ATPase subunit 6. Cell 1990;61:885–94. [PubMed: 2140530]

5. Feagin JE, Shaw JM, Simpson L, et al. Creation of AUG initiation codons by addition of uridines within cytochrome b transcripts of kinetoplastids. Proc Natl Acad Sci USA 1988;85:539–43. [PubMed: 2448777]

6. Koslowsky DJ, Bhat GJ, Perrollaz AL, et al. The MURF3 gene of *T. brucei* contains multiple domains of extensive editing and is homologous to a subunit of NADH dehydrogenase. Cell 1990;62:901–11. [PubMed: 2393904]

7. Shaw J, Feagin JE, Stuart K, et al. Editing of mitochondrial mRNAs by uridine addition and deletion generates conserved amino acid sequences and AUG initiation codons. Cell 1988;53:401–11. [PubMed: 2452696]

8. Corell RA, Myler P, Stuart K. *Trypanosoma brucei* mitochondrial CR4 gene encodes an extensively edited mRNA with completely edited sequence only in bloodstream forms. Mol Biochem Parasitol 1994;64:65–74. [PubMed: 8078524]

9. Read LK, Myler PJ, Stuart K. Extensive editing of both processed and preprocessed maxicircle CR6 transcripts in *Trypanosoma brucei*. J Biol Chem 1992;267:1123–8. [PubMed: 1730639]

10. Read LK, Wilson KD, Myler PJ, et al. Editing of *Trypanosoma brucei* maxicircle CR5 mRNA generates variable carboxy terminal predicted protein sequences. Nucleic Acids Res 1994;22:1489–95. [PubMed: 7514788]

11. Maslov DA, Nawathean P, Scheel J. Partial kinetoplast-mitochondrial gene organization and expression in the respiratory deficient plant trypanosomatid *Phytomonas serpens*. Mol Biochem Parasitol 1999;99:207–21. [PubMed: 10340485]

12. Maslov DA, Simpson L. RNA editing and mitochondrial genomic organization in the cryptobiid kinetoplastid protozoan, *Trypanoplasma borreli*. Mol Cell Biol 1994;14:8174–82. [PubMed: 7969154]

13. Landweber LF, Gilbert W. RNA editing as a source of genetic variation. Nature 1993;363:179–82. [PubMed: 8387160]

14. Chugunov VA, Shirshov AT, Zaitseva GN. A comparative study of the ribosomes from kinetoplasts and cytoplasm of the zooflagellate, *Strigomonas oncopelt*i. Biokhimiya (in Russian) 1971;36:630–5.

15. Hanas J, Linden G, Stuart K. Mitochondrial and cytoplasmic ribosomes and their activity in blood and culture form *Trypanosoma brucei*. J Cell Biol 1975;65:103–11. [PubMed: 1127006]

16. Shu HH, Göringer HU. *Trypanosoma brucei* mitochondrial ribonucleoprotein complexes which contain 12S and 9S ribosomal RNAs. Parasitology 1998;116:157–64. [PubMed: 9509025]

17. Tittawella I, Yasmin L, Baranov V. Mitochondrial ribosomes in a trypanosome. Biochem Biophys Res Commun 2003;307:578–83. [PubMed: 12893262]

18. Eperon I, Janssen J, Hoeijmakers J, et al. The major transcripts of the kinetoplast DNA of *T. bruce*i are very small ribosomal RNAs. Nucl Acids Res 1983;11:105–25. [PubMed: 6306559]

19. de la Cruz V, Lake JA, Simpson AM, et al. A minimal ribosomal RNA: Sequence and secondary structure of the 9S kinetoplast ribosomal RNA from *Leishmania tarentola*e. Proc Natl Acad Sci USA 1985;82:1401–5. [PubMed: 3856267]

20. de la Cruz V, Simpson A, Lake J, et al. Primary sequence and partial secondary structure of the 12S kinetoplast (mitochondrial) ribosomal RNA from *Leishmania tarentolae*: Conservation of peptidyl-transferase structural elements. Nucl Acids Res 1985;13:2337–56. [PubMed: 2987850]

21. Pel HJ, Grivell LA. Protein synthesis in mitochondria. Mol Biol Rep 1994;19:183–94. [PubMed: 7969106]

22. Maslov DA, Sharma MR, Butler E, et al. Isolation and characterization of mitochondrial ribosomes and ribosomal subunits from *Leishmania tarentolae*. Mol Biochem Parasitol 2006;148:69–78. [PubMed: 16600399]

23. Laemmli UK. Cleavage of structural proteins during the assembly of the head of bacteriophage T4. Nature 1970;227:680–5. [PubMed: 5432063]

24. Sambrook, J.; Fritsch, EF.; Maniatis, T. Molecular Cloning - a laboratory manual. 2 ed.. Cold Spring Harbor Laboratory Press; 1989.

25. Perkins DN, Pappin DJ, Creasy DM, Cottrell JS. Probability-based protein identification by searching sequence databases using mass spectrometry data. Electrophoresis 1999;20:3551–67. [PubMed: 10612281]

26. Pappin DJC, Hojrup P, Bleasby AJ. Rapid identification of proteins by peptide-mass fingerprinting. Curr Biol 1993;3:327–32. [PubMed: 15335725]

27. Wagenknecht T, Grassucci R, Frank J. Electron microscopy and computer image averaging of ice-embedded large ribosomal subunits from *Escherichia coli*. J Mol Biol 1988;199:137–47. [PubMed: 2451023]

28. Frank J, Bretaudiere JP, Carazo JM, et al. Classification of images of biomolecular assemblies: a study of ribosomes and ribosomal subunits of *Escherichia col*i. J Microsc 1988;150(Pt 2):99–115. [PubMed: 3045323]

29. Frank J, Radermacher M, Penczek P, et al. SPIDER and WEB: processing and visualization of images in 3D electron microscopy and related fields. J Struct Biol 1996;116:190–9. [PubMed: 8742743]

30. Spedding, G. Isolation and analysis of ribosomes from prokaryotes, eukaryotes and organelles. In: Spedding, G., editor. Ribosomes and protein synthesis - A practical approach. IRL Press; 1990. p. 1-29.

31. Sharma MR, Koc EC, Datta PP, et al. Structure of the mammalian mitochondrial ribosome reveals an expanded functional role for its component proteins. Cell 2003;115:97–108. [PubMed: 14532006]

32. Suzuki T, Terasaki M, Takemoto-Hori C, et al. Proteomic analysis of the mammalian mitochondrial ribosome - Identification of protein components in the 28 S small subunit. J Biol Chem 2001;276:33181–95. [PubMed: 11402041]

33. Koc EC, Burkhart W, Blackburn K, et al. The small subunit of the mammalian mitochondrial ribosome - Identification of the full complement of ribosomal proteins present. J Biol Chem 2001;276:19363–74. [PubMed: 11279123]

34. Kitakawa M, Graack HR, Grohmann L, et al. Identification and characterization of the genes for mitochondrial ribosomal proteins of *Saccharomyces cerevisiae*. Eur J Biochem 1997;245:449–56. [PubMed: 9151978]

35. O'Brien TW. Properties of human mitochondrial ribosomes. IUBMB Life 2003;55:505–13. [PubMed: 14658756]

36. Suzuki T, Terasaki M, Takemoto-Hori C, et al. Structural compensation for the deficit of rRNA with proteins in the mammalian mitochondrial ribosome - Systematic analysis of protein components of the large ribosomal subunit from mammalian mitochondria. J Biol Chem 2001;276:21724–36. [PubMed: 11279069]

37. Koc EC, Burkhart W, Blackburn K, et al. The large subunit of the mammalian mitochondrial ribosome - Analysis of the complement of ribosomal proteins present. J Biol Chem 2001;276:43958–69. [PubMed: 11551941]

38. Koc EC, Burkhart W, Blackburn K, et al. A proteomics approach to the identification of mammalian mitochondrial small subunit ribosomal proteins. J Biol Chem 2000;275:32585–91. [PubMed: 10938081]

39. Gan X, Kitakawa M, Yoshino K, et al. Tag-mediated isolation of yeast mitochondrial ribosome and mass spectrometric identification of its new components. Eur J Biochem 2002;269:5203–14. [PubMed: 12392552]

40. Gan X, Arita K, Isono S, et al. Identification and comparative analysis of the large subunit mitochondrial ribosomal proteins of *Neurospora crass*a. FEMS Microbiol Lett 2006;254:157–64. [PubMed: 16451194]

41. Yamaguchi K, Subramanian AR. The plastid ribosomal proteins - Identification of all the proteins in the 50 S subunit of an organelle ribosome (chloroplast). J Biol Chem 2000;275:28466–82. [PubMed: 10874046]

42. Yamaguchi K, Von Knoblauch K, Subramanian AR. The plastid ribosomal proteins - Identification of all the proteins in the 30 S subunit of an organelle ribosome (chloroplast). J Biol Chem 2000;275:28455–65. [PubMed: 10874039]

43. Maslov DA, Sturm NR, Niner BM, et al. An intergenic G-rich region in *Leishmania tarentolae* kinetoplast maxicircle DNA is a pan-edited cryptogene encoding ribosomal protein S12. Mol Cell Biol 1992;12:56–67. [PubMed: 1370342]

44. Lurin C, Andres C, Aubourg S, et al. Genome-wide analysis of *Arabidopsis* pentatricopeptide repeat proteins reveals their essential role in organelle biogenesis. Plant Cell 2004;16:2089–103. [PubMed: 15269332]

45. Mingler MK, Hingst AM, Clement SL, et al. Identification of pentatricopeptide repeat proteins in *Trypanosoma bruce*i. Mol Biochem Parasitol 2006;150:37–45. [PubMed: 16837079]

46. Missel A, Souza AE, Nörskau G, et al. Disruption of a gene encoding a novel mitochondrial DEAD-box protein in *Trypanosoma brucei* affects edited mRNAs. Mol Cell Biol 1997;17:4895–903. [PubMed: 9271369]

47. Mazumder R, Iyer LM, Vasudevan S, et al. Detection of novel members, structure-function analysis and evolutionary classification of the 2H phosphoesterase superfamily. Nucleic Acids Res 2002;30:5229–43. [PubMed: 12466548]

48. Fraser ID, Tavalin SJ, Lester LB, et al. A novel lipid-anchored A-kinase Anchoring Protein facilitates cAMP-responsive membrane events. EMBO J 1998;17:2261–72. [PubMed: 9545239]

49. Lee I, Bender E, Kadenbach B. Control of mitochondrial membrane potential and ROS formation by reversible phosphorylation of cytochrome *c* oxidase. Mol Cell Biochem 2002;234-235:63–70. [PubMed: 12162461]

50. Ko YH, Pan W, Inoue C, et al. Signal transduction to mitochondrial ATP synthase: evidence that PDGF-dependent phosphorylation of the delta-subunit occurs in several cell lines, involves tyrosine, and is modulated by lysophosphatidic acid. Mitochondrion 2002;1:339–48. [PubMed: 16120288]

51. Lee I, Salomon AR, Ficarro S, et al. cAMP-dependent tyrosine phosphorylation of subunit I inhibits cytochrome c oxidase activity. J Biol Chem 2005;280:6094–100. [PubMed: 15557277]
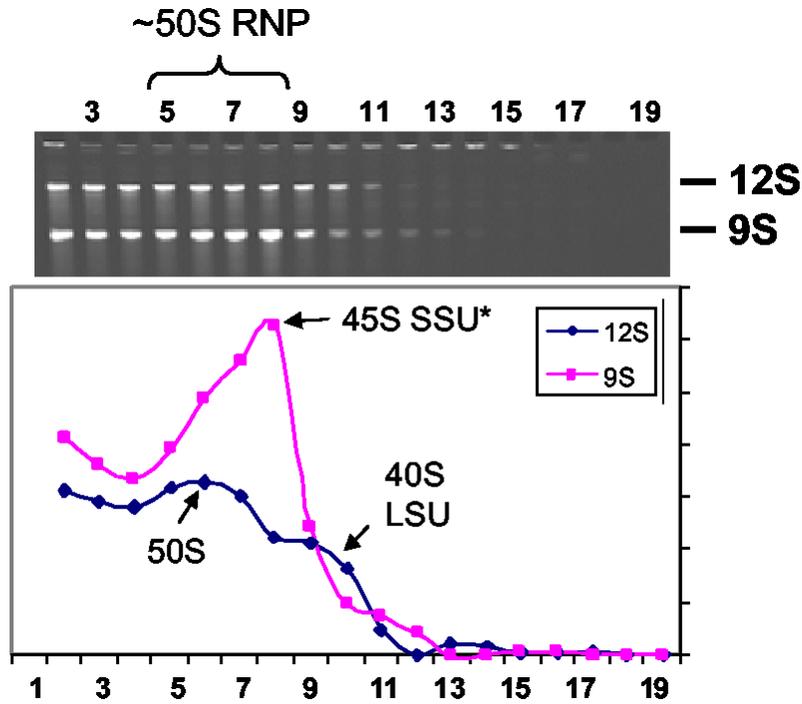
Fig 1.
Ribosomal ribonucleoprotein complexes in mitochondrial lysates of *L. tarentolae* obtained after sedimentation through 1.1 M sucrose cushion. The upper panel shows the ethidium bromide staining profiles of the 9S and 12S rRNAs obtained from complexes fractionated in a 7-30% sucrose gradient (SW28 rotor, 20,000 rpm, 16 h) following electrophoretic separation in a 4% polyacrylamide-urea gel The lower panel shows the RNA content of individual fractions in arbitrary units derived from integrative optical density (IOD) of the fluorescence of the rRNA in the gel.
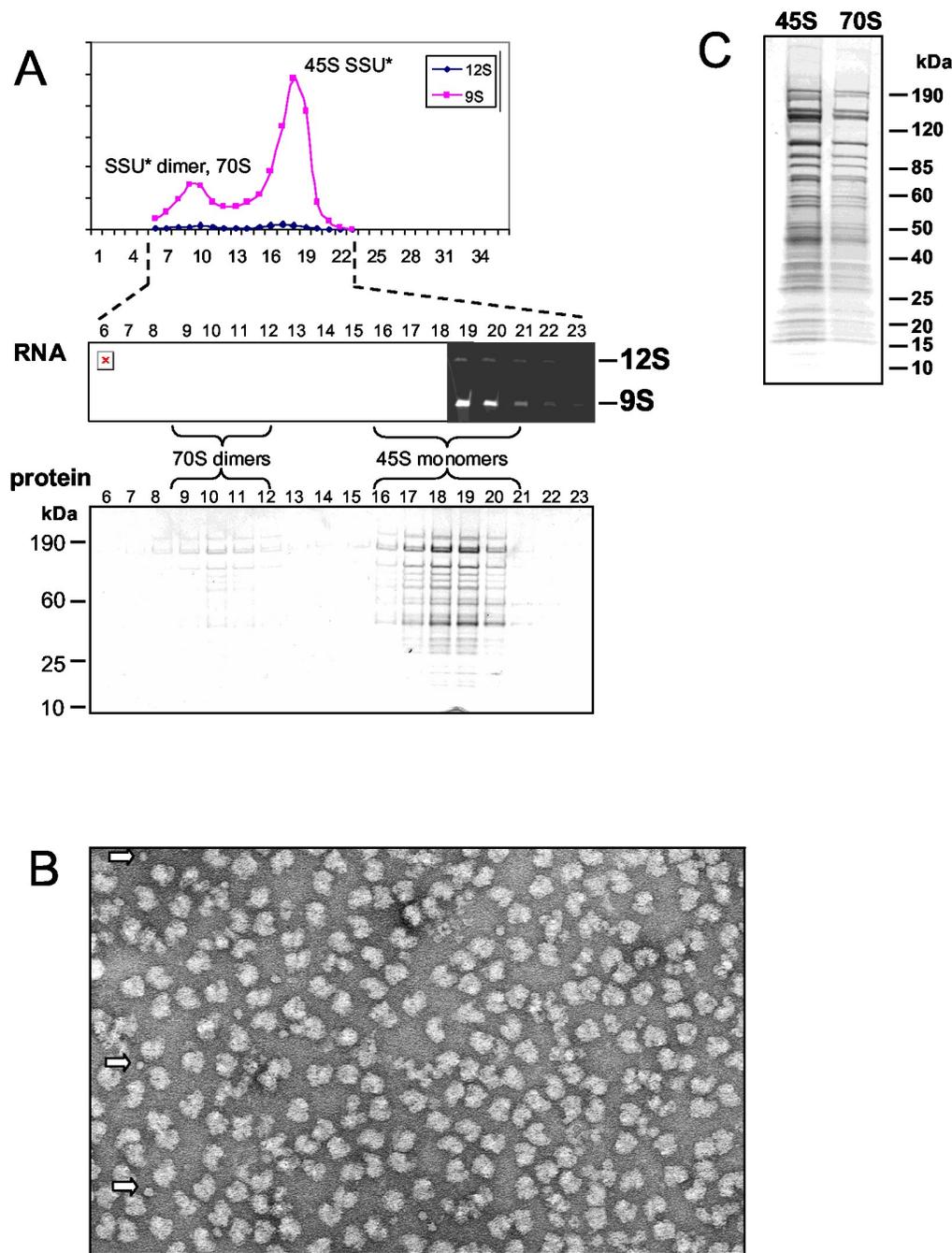
Fig 2.
Isolation of monomeric and dimeric 45S complexes under normal (100 mM KCl, 10 mM MgCl$_2$) conditions. The SSU* particles were recovered from the gradient shown in Fig. 1 by sedimentation and then fractionated in a second 7-30% sucrose gradient (SW41 rotor, 20,000 rpm, 16 h): (A) the 9S and 12S RNA profile is shown in the upper and middle panels and the corresponding protein profile is shown in the lower panel; (B) transmission electron microscopy of uranyl acetate stained particles from the monomeric 45S complexes with the white arrows pointing at the smaller particles possibly representing ATP synthase; (C) proteins in the purified monomeric (45S) and dimeric (70S) SSU* complexes separated in a 8-16% polyacrylamide Tris-glycine-SDS polyacrylamide gel and stained with Coomassie Blue.
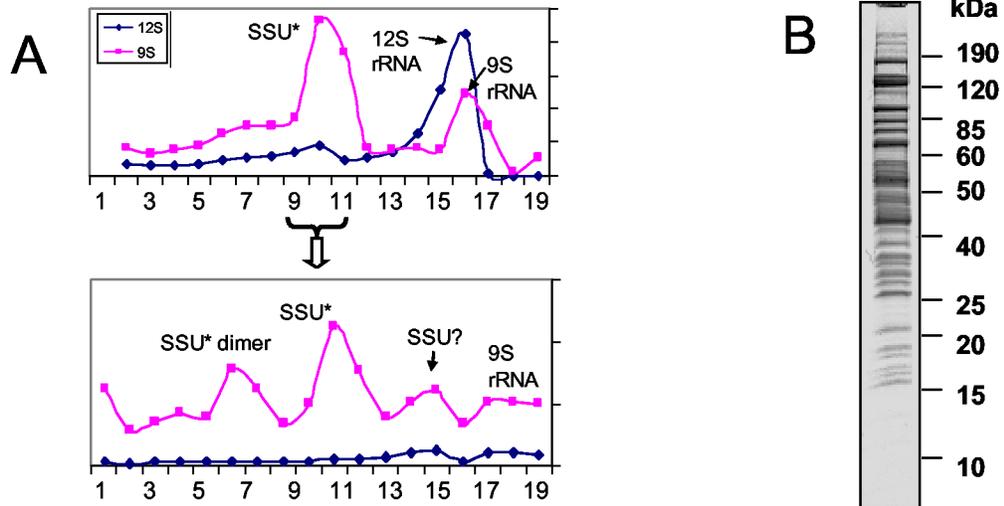
Fig 3.
Isolation of salt-washed 45S SSU* complexes: (A) following the centrifugation of the mitochondrial lysate through a sucrose cushion, the pelleted ribosomal RNP complexes were resuspended and fractionated on a 7-30% sucrose gradient containing 1.5 M KCl (SW41 rotor, 23,000 rpm, 16 h). The presence of the 9S and 12S rRNAs was determined by gel electrophoresis as described in Materials and Methods (upper panel). The 45S complexes from fractions 9-11 were recovered by sedimentation and fractionated on a second sucrose gradient (lower panel) containing 1.5 M KCl (SW41 rotor, 23,000 rpm, 16 h); (B) proteins of the complexes recovered from the second gradient after separation in a 8-16% polyacrylamide Tris-glycine-SDS polyacrylamide gel and staining with Coomassie Blue.
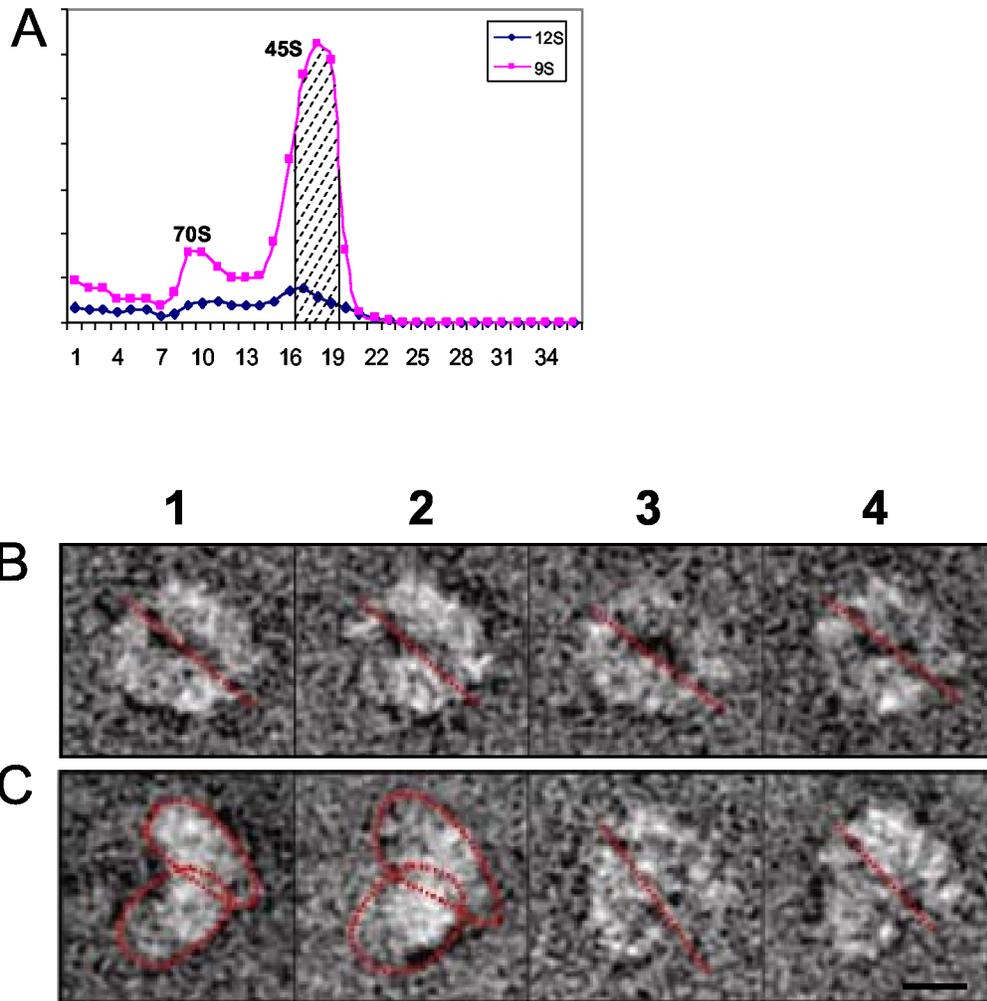
Fig 4.

Cryo-EM of the 45S SSU* complexes: (A) Second round of sedimentation of the 45S
complexes through a 7-30% sucrose gradient (SW41, 20,000 rpm, 16 h). Particles from the
fractions representing the main 45S peak (indicated by shading) were recovered by pelleting
and used for cryo-EM. (B) Representative 2D averages showing two SSUs situated side-by-
side. Red dashed lines indicate the boundaries between the two putative SSUs. (C)
Representative 2D averages, showing the bilobed feature. In panels C1 and C2, tentative
boundaries of the two overlapping SSUs are indicated by red dashed lines. Panels C3 and C4
show averages with asymmetric bilobed features. Red dashed lines are to indicate boundaries
between the two lobes. The right-side lobe can be identified as a SSU. Scale bar is 100Å.

Table 1

Polypeptides associated with mitochondrial ribosomal 45S SSU* complexes

L. major GeneDB id	Size kDa	Homology, domains, misc. features (E-score)	pI	45S preparation used / peptides found		
				monomeric	dimeric	salt washed
High confidence hits:						
LmjF16.1230	199.5	Coiled coil	8.84	15	12	9
LmjF22.0990	139.0		6.25	4	4	1
LmjF27.1895	133.0		6.69	9	7	4
LmjF27.0630	99.4	Coiled coil	9.01	3	3	2
LmjF24.0830	94.4	PPR	9.10	11	10	6
LmjF33.0010	92.4	Coiled coil	5.73	2	4	3
LmjF15.0410	77.7	PPR	6.19	5	6	8
LmjF33.2510	75.4		9.20	6	5	4
LmjF35.3940	73.0		9.15	5	3	5
LmjF15.0780	72.1		9.42	10	12	5
LmjF29.0430	65.0	PPR	9.18	7	6	4
LmjF12.0040	54.2	MRPS29 (9e-12)	8.30	4	4	2
LmjF20.0510	50.3	S15 (0.009)	10.01	7	8	3
LmjF35.3490	49.5	Coiled coil	9.17	9	10	2
LmjF36.1860	49.3	S5 (4e-08)	9.77	7	7	2
LmjF30.0650	45.7		9.27	4	1	4
LmjF30.3220	43.5		6.36	2	3	1
LmjF05.0340	40.9	S11 (0.51)	9.64	4	4	1
LmjF23.1190	39.5	S9 (0.12)	6.51	5	6	2
LmjF36.2310	37.7	S18 (weak)	10.01	3	5	3
LmjF15.0080	36.7		6.17	3	3	2
LmjF03.0630	36.0		7.91	3	2	1
LmjF35.3850	36.0	S17 (2e-09)	9.76	7	4	2
LmjF03.0220	35.7		10.24	3	3	1
LmjF22.0830	35.1		10.05	5	3	2
LmjF18.0800	35.0	S8 (8e-04)	9.55	3	3	4
LmjF15.1400	33.8	Coiled coil	5.23	2	3	2
LmjF35.2230	33.4		8.92	4	3	2
LmjF32.0650	31.4	part. LigT (2e-04)	9.19	1	1	4
LmjF30.3530	30.1	RHOD (5e-05)	6.68	1	1	2
LmjF26.2270	29.2		5.73	5	3	4
LmjF28.2180	27.4		5.66	4	4	1
LmjF25.2160	27.3	Ubiquitin-like	5.03	4	4	1
LmjF28.0920	22.4	S16 (0.038)	10.00	3	4	6
LmjF36.4120	21.5		10.95	3	4	5
LmjF27.0180	20.9		8.95	4	4	4
LmjF30.0740	19.6		10.59	4	2	1
LmjF22.1220	19.4		10.55	3	4	3
LmjF34.0400	18.7	S6 (1.0)	9.16	2	1	6
Additional possible components:						
LmjF24.0800	66.0		9.47	1	1	
LmjF32.0570	64.2	DEAD/H-box helicase (1e-80)	9.64	1	1	
LmjF30.2660	56.4	TPR (0.034)	9.73	1	1	1
LmjF18.0320	44.3		9.64	1	1	
LmjF08.1100	42.0		8.24	1	2	
LmjF08.0120	30.3		9.57	1		2
LmjF21.0827	24.3		9.55	4	3	
LmjF29.1540	22.8		10.99		1	1
LmjF28.2980	19.8		9.98	2	2	
LmjF30.3235	11.5		6.20	1	1	

L. major	Size	Homology, domains,	pI	45S preparation used / peptides found		
		misc. features (E-score)				
GeneDB id	kDa			monomeric	dimeric	salt washed